

Noninvasive Assessment of Neuromechanical and Neuroventilatory Coupling in COPD

Manuel Lozano-García ¹, Luis Estrada-Petrocelli ¹, *Senior Member, IEEE*, Dolores Blanco-Almazán ¹, Basak Tas, Peter S. P. Cho, John Moxham ², Gerrard F. Rafferty ², Abel Torres ², *Senior Member, IEEE*, Raimon Jané ¹, *Senior Member, IEEE*, and Caroline J. Jolley ¹

Abstract—This study explored the use of parasternal second intercostal space and lower intercostal space surface electromyogram (sEMG) and surface mechanomyography (sMMG) recordings (sEMG_{para} and sMMG_{para}, and sEMG_{lic} and sMMG_{lic}, respectively) to assess neural respiratory drive (NRD), neuromechanical (NMC) and neuroventilatory (NVC) coupling, and mechanical efficiency (MEff) noninvasively in healthy subjects and chronic obstructive pulmonary disease (COPD) patients. sEMG_{para}, sMMG_{para}, sEMG_{lic}, sMMG_{lic}, mouth pressure (P_{mo}), and volume (V_i) were measured at rest, and during an inspiratory loading protocol, in 16 COPD patients (8 moderate and 8 severe) and 9 healthy subjects. Myographic signals were analyzed using fixed sample entropy and normalized to their largest values (fSEsEMG_{para%max}, fSEsMMG_{para%max}, fSEsEMG_{lic%max}, and fSEsMMG_{lic%max}). fSEsMMG_{para%max}, fSEsEMG_{para%max}, and fSEsEMG_{lic%max} were significantly higher in COPD than in healthy participants at rest. Parasternal intercostal muscle NMC was significantly higher in healthy than in COPD participants at rest, but not during threshold loading. P_{mo}-derived NMC and MEff ratios were lower in severe patients than in mild patients or healthy subjects during threshold loading, but differences were not consistently significant. During resting breathing and threshold loading, V_i-derived NVC and MEff ratios were significantly lower in severe patients than in mild patients or healthy subjects. sMMG is a potential noninvasive alternative to sEMG for assessing NRD in COPD. The ratios of P_{mo} and V_i to sMMG and sEMG measurements provide wholly noninvasive NMC, NVC, and MEff indices that are sensitive to impaired respiratory mechanics in COPD and are therefore of potential value to assess disease severity in clinical practice.

Index Terms—Chronic obstructive pulmonary disease, disease severity, electromyography, healthy volunteers, mechanomyography, respiratory mechanics, respiratory muscles.

I. INTRODUCTION

ASSESSMENT of respiratory muscle function provides insights into the physiological basis of breathlessness and disease severity in chronic respiratory diseases, such as chronic obstructive pulmonary disease (COPD) [1]. The clinical utility of neural respiratory drive (NRD) and neuromechanical coupling (NMC) indices derived from measures of esophageal crural diaphragm electromyogram (oesEMG_{di}) and transdiaphragmatic pressure (P_{di}) is however limited by the invasiveness of these measurements, the discomfort for patients, and the need for special training of physicians. Surface electromyography (sEMG) recorded over the parasternal second intercostal space (sEMG_{para}) and over lower intercostal spaces (sEMG_{lic}) provides a robust measure of the load on the respiratory muscles, and therefore an alternative, wholly noninvasive, measure of NRD in laboratory and clinical settings [2]–[6]. Additionally, surface mechanomyography (sMMG) recorded over the parasternal second intercostal space (sMMG_{para}) and over lower intercostal spaces (sMMG_{lic}), using accelerometers on the skin surface, represents inspiratory muscle fiber vibration during contraction and has been proposed to provide noninvasive indices of inspiratory muscle force generation [6]–[9]. The use of sEMG_{para}, sMMG_{para}, sEMG_{lic}, and sMMG_{lic} signals, together with measurements of mouth pressure (P_{mo}) and volume (V_i), to obtain noninvasive indices of NMC, neuroventilatory coupling (NVC), and mechanical efficiency (MEff) has been evaluated in healthy subjects [9], [10] but not in COPD patients.

The aim of the present study was to explore the use of sEMG_{para}, sMMG_{para}, sEMG_{lic}, and sMMG_{lic} recordings to assess and compare levels of NRD, NMC, NVC, and MEff measured noninvasively in a sample of healthy subjects and COPD patients.

We hypothesized that measurements of sEMG_{para}, sEMG_{lic}, sMMG_{para}, and sMMG_{lic} would be higher in COPD patients compared to healthy controls and inversely related to airflow obstruction, reflecting increased respiratory muscle activation. We furthermore hypothesized that the corresponding

Manuscript received September 8, 2021; revised February 25, 2022; accepted April 2, 2022. Date of publication April 11, 2022; date of current version July 4, 2022. This work was supported in part by the Generalitat de Catalunya through CERCA Program, under Grant GRC 2017 SGR 01770, in part by the Gobierno de España under Grant RTI2018-098472-B-I00 MCIU/AEI/FEDER, UE, and in part by the Biomedical Research Networking Centre in Bioengineering, Biomaterials and Nanomedicine (CIBER-BBN), Instituto de Salud Carlos III/FEDER. The work of Manuel Lozano-García was supported by the European Respiratory Society Fellowship under Grant ERS LTRF 2015-5185. The work of Luis Estrada-Petrocelli was supported by European Respiratory Society Fellowship under Grant ERS LTRF 2017 01-00086. (Raimon Jané and Caroline J. Jolley contributed equally to this work.) (Corresponding author: Manuel Lozano-García.)

Please see the Acknowledgment section of this article for the author affiliations.

Digital Object Identifier 10.1109/JBHI.2022.3166255

noninvasive indices of NMC, NVC, and MEff would be lower in COPD patients than in healthy controls.

II. METHODOLOGY

A. Ethics Statement

This prospective observational study was granted research ethics committee approval (NRES Committee London – Dulwich 05/Q0703) and was conducted in accordance with the principles of the Declaration of Helsinki at a single center (King’s College Hospital, London, United Kingdom). All subjects provided their written consent before participation.

B. Study Subjects

COPD patients were recruited prospectively from an outpatient clinic. All had a clinician diagnosis of COPD (≥ 10 -pack year smoking history and forced expiratory volume in 1 second (FEV₁) to forced vital capacity (FVC) ratio < 0.7) [11] and were clinically stable without COPD exacerbation within the preceding 6 weeks. Healthy subjects were recruited by advertisement.

C. Measurements

Post-bronchodilator spirometry (FEV₁, FVC, and FEV₁/FVC ratio) was measured in all subjects in accordance with standard clinical guidelines [12]. FEV₁ and FVC values were expressed as percentages of predicted values (FEV₁% predicted and FVC % predicted, respectively) calculated with reference to Global Lung Function Initiative (GLI-2012) prediction equations [13]. COPD patients were sub-classified into two groups based on FEV₁: COPD_{>50} (FEV₁ ≥ 50 % predicted, $n = 8$) and COPD_{<50} (FEV₁ < 50 % predicted, $n = 8$). Dyspnea was assessed in all patients using the modified British Medical Research Council (mMRC) dyspnea scale [14].

sEMG_{para} and sEMG_{lic} were recorded using surface electrodes, one pair placed over the second intercostal space bilaterally (sEMG_{para}) [2], [15], and the other pair placed over the seventh or eighth right intercostal spaces, between the mid-axillary and the anterior axillary lines (sEMG_{lic}) [6], [16]. sMMG_{para} and sMMG_{lic} were recorded using two triaxial accelerometers attached to the skin with adhesive rings, one over the second intercostal space on the right (sMMG_{para}), and another close to the sEMG_{lic} electrodes over the lower intercostal spaces (sMMG_{lic}) [6], [7]. Airflow was measured with a pneumotachograph and P_{mo} was measured with a differential pressure transducer connected to a side port of the pneumotachograph. All signals were recorded continuously during all stages of the protocol.

D. Study Protocol

1) *Maximal Inspiratory Maneuvers*: First, all subjects performed a maximal static inspiratory pressure maneuver against an occluded mouthpiece [1] (P_{Imax}), and a maximal inspiration to total lung capacity [2], [17]. These maneuvers were repeated several times to ensure maximal volitional effort. Subjects were sitting upright with a nose clip.

2) *Inspiratory Threshold Loading Protocol*: After the maximal inspiratory maneuvers, all subjects performed an inspiratory threshold loading protocol. Inspiratory threshold loads of 12 %, 24 %, 36 %, 48 %, and 60 % of the subject’s P_{Imax} were generated with an electronic inspiratory muscle trainer (POWERbreathe K5; POWERbreathe International Ltd, Southam, U.K.) connected to the pneumotachograph. Subjects were sitting with a nose clip and breathed through a mouthpiece attached to the pneumotachograph. First, baseline measurements were recorded for a minimum of 2 min of resting breathing. Then, the POWERbreathe was connected to the pneumotachograph and the threshold loads were imposed. At each load, 30 breaths were performed and followed by a short resting period. Subjects rated their breathlessness intensity on the modified Borg scale (mBorg) at the end of each load [18].

E. Data Analysis

1) *Calculation of Myographic Fixed Sample Entropy Time-Series*: The three mechanomyographic signals provided by each triaxial accelerometer were root sum squared to obtain one mechanomyographic vector magnitude signal. The amplitude of all myographic signals was then analyzed using fixed sample entropy (fSampEn), a technique that can track amplitude variations of a signal with the advantage of being very robust to cardiac artifacts, as previously described [5]–[7]. sEMG_{para}, sEMG_{lic}, and vector magnitude sMMG_{para} and sMMG_{lic} signals were converted to fSampEn using the fSampEn parameters proposed in [19], thus obtaining fSEsEMG_{para}, fSEsEMG_{lic}, fSEsMMG_{para}, and fSEsMMG_{lic} time-series.

2) *Calculation of Neuromechanical and Neuroventilatory Coupling and Mechanical Efficiency Parameters*: The respiratory phases were identified using a zero-crossing detector on the P_{mo} signal. All signals were visually examined and respiratory cycles containing unusual pressure patterns or low quality myographic signals were rejected. Ten cycles were automatically selected, as previously described [6], for resting breathing and each inspiratory threshold load, resulting in 60 cycles for each subject. Mean inspiratory P_{mo} and area under the curve of the inspiratory flow trace (inspiratory volume V_i) were calculated for each cycle. The level of inspiratory muscle activity was calculated for each cycle as the inspiratory mean fSEsEMG_{para}, fSEsEMG_{lic}, fSEsMMG_{para}, and fSEsMMG_{lic}. These values were expressed as percentages of the respective largest values obtained during either the inspiratory threshold loading protocol, the P_{Imax} maneuver, or the inspiratory lung capacity maneuver (fSEsEMG_{para%max}, fSEsEMG_{lic%max}, fSEsMMG_{para%max}, and fSEsMMG_{lic%max}).

NMC indices were calculated as in:

$$NMC_{MMG-para} = \frac{fSEsMMG_{para\%max}}{fSEsEMG_{para\%max}} \quad (1)$$

$$NMC_{MMG-lic} = \frac{fSEsMMG_{lic\%max}}{fSEsEMG_{lic\%max}} \quad (2)$$

$$NMC_{P-para} = \frac{mean P_{mo}}{fSEsEMG_{para\%max}} \quad (3)$$

$$NMC_{P-lic} = \frac{\text{mean } P_{mo}}{fSEsEMG_{lic\%max}} \quad (4)$$

NVC indices were calculated as in:

$$NVC_{para} = \frac{V_i}{fSEsEMG_{para\%max}} \quad (5)$$

$$NVC_{lic} = \frac{V_i}{fSEsEMG_{lic\%max}} \quad (6)$$

MEff indices were calculated as in:

$$MEff_{P-para} = \frac{\text{mean } P_{mo}}{fSEsMMG_{para\%max}} \quad (7)$$

$$MEff_{P-lic} = \frac{\text{mean } P_{mo}}{fSEsMMG_{lic\%max}} \quad (8)$$

$$MEff_{V-para} = \frac{V_i}{fSEsMMG_{para\%max}} \quad (9)$$

$$MEff_{V-lic} = \frac{V_i}{fSEsMMG_{lic\%max}} \quad (10)$$

Coupling indices, as in (1)-(6), described relationships between the electrical activation of inspiratory muscles, represented by sEMG, and the resulting mechanical output, represented by either sMMG, P_{mo} or V_i . These indices therefore involved measures of different nature and represented how well myoelectrical activation was translated into a mechanical response. Efficiency indices, as in (7)-(10), described however relationships between two measures of the same nature, i.e., two mechanical measures, and represented how efficient was the translation of the mechanical activation of inspiratory muscles into global mechanical output.

The median values of all parameters were calculated for the ten cycles of resting breathing and each inspiratory threshold load.

Data were analyzed in MATLAB (The MathWorks, Inc., vR2020a, Natick, MA, USA).

F. Statistical Analysis

All data are expressed as median and interquartile range. Comparison of anthropometric and clinical data of healthy subjects, COPD_{>50} patients, and COPD_{<50} patients was made using Kruskal-Wallis tests, followed by multiple pairwise comparisons with Tukey-Kramer adjusted p-values.

Measures of respiratory pressures, breathing pattern, breathlessness, and inspiratory muscle activity were analyzed using linear mixed models. Three models were defined for each measure, all with group (healthy, COPD_{>50} or COPD_{<50}), load, and the interaction between group and load as fixed effects. Regarding by-subject random effects, one model was defined with random intercepts, another with correlated random intercepts and random slopes for load, and a third one with uncorrelated random intercepts and random slopes for load. The model with the lowest Akaike information criterion (AIC) value was selected, and the standardized Pearson residuals were used to detect outliers. All three models were then refitted with outliers excluded, and again the model with the lowest AIC value was

selected as the best model. The statistical significance of all coefficients representing each fixed effect was tested using an F-test. Significant interactions between group and load factors, and significant group factor effects were followed by multiple pairwise F-tests with Benjamini-Hochberg-adjusted p-values to determine which groups were different at each load level and across loads.

Relationships between FEV₁ and measurements of resting inspiratory muscle activity, and between sEMG- and sMMG-derived measures of NRD, NMC, NVC, and MEff were analyzed by simple linear regression analysis.

III. RESULTS

Sixteen COPD patients and nine healthy controls were studied. Anthropometric and clinical data are summarized in Table I.

A. Respiratory Pressures, Breathing Pattern, and Breathlessness

PI_{max} was significantly lower in the COPD_{<50} patients (33.0 (29.8-38.2) cmH₂O) compared to both the healthy subjects (64.0 (53.0-81.0) cmH₂O, p = 0.02) and COPD_{>50} patients (71.0 (51.2-81.2) cmH₂O, p = 0.02). Reflecting these baseline differences in PI_{max}, the peak P_{mo} generated during the inspiratory threshold loading protocol was significantly lower in the COPD_{<50} patients than in the COPD_{>50} and healthy control groups across inspiratory loads (Fig. 1a).

V_i was significantly lower in the COPD_{<50} patients than in the COPD_{>50} and healthy control groups from 12 % to 60 % PI_{max} (Fig. 1b). V_i was also significantly lower in the COPD_{>50} than in the healthy control group at the two highest inspiratory loads. COPD patients reported significantly higher mBorg breathlessness intensity values than healthy subjects throughout the inspiratory threshold loading protocol (Fig. 1c).

B. Measurements of Inspiratory Muscle Activity

Representative recordings in a healthy subject and a COPD patient are shown in Fig. 2.

1) *Inspiratory Muscle Activity At Rest*: During resting breathing fSEsMMG_{para%max} was significantly higher in COPD_{<50} (26.1 (18.3-30.8) %, p = 0.046) and COPD_{>50} (22.2 (14.8-33.1) %, p = 0.046) patients compared to healthy subjects (15.5 (12.5-17.5) %). fSEsEMG_{para%max} and fSEsEMG_{lic%max} were also significantly higher during resting breathing in COPD_{<50} (36.5 (24.2-41.1) % and 29.2 (26.8-35.7) %, respectively) (p < 0.001) and COPD_{>50} (23.3 (19.1-30.2) %, p = 0.01, and 23.3 (13.3-43.4) %, p = 0.03, respectively) patients than in healthy subjects (10.1 (7.2-13.8) % and 10.3 (6.9-14.0) %, respectively). Although resting fSEsMMG_{lic%max} values were lower in healthy subjects, there were no statistically significant differences between groups.

There were statistically significant negative correlations between FEV₁% predicted and resting fSEsEMG_{para%max} (r = -0.68, p < 0.001), resting fSEsEMG_{lic%max} (r = -0.61, p =

TABLE I
ANTHROPOMETRIC AND CLINICAL DATA FOR HEALTHY SUBJECTS AND COPD PATIENTS

	Healthy subjects	COPD _{>50} patients	COPD _{<50} patients	p-value
Number of subjects	9	8	8	
Male (%)	55.6	75.0	62.5	
Age (yrs)	64 (63-67)	70 (65-73)	66 (63-68)	0.28
BMI (kg/m ²)	24.3 (23.8-29.0)	27.6 (23.4-29.5)	25.1 (20.2-26.2)	0.62
FEV ₁ (% predicted)	112.9 (107.3-114.4) **	56.2 (55.2-64.0) #	34.5 (33.2-40.0) *	<0.001
FVC (% predicted)	116.4 (108.5-121.0) *	104.4 (95.1-109.1)	84.4 (80.7-94.9) *	0.02
FEV ₁ /FVC (%)	79.3 (74.4-82.4) **	45.2 (37.3-51.6) #	30.1 (28.5-39.7) *	<0.001
mMRC grade	NA	2.0 (2.0-3.5)	2.5 (1.0-3.0)	0.80

Data are expressed as median (interquartile range).

BMI = body mass index, COPD_{>50} = chronic obstructive pulmonary disease patients with a forced expiratory volume in 1 second value greater than or equal to 50 % predicted, COPD_{<50} = chronic obstructive pulmonary disease patients with a forced expiratory volume in 1 second value lower than 50 % predicted, FEV₁ = forced expiratory volume in 1 second, FVC = forced vital capacity, mMRC = modified British Medical Research Council, * or # = p-value < 0.05. Spirometry was performed after bronchodilation.

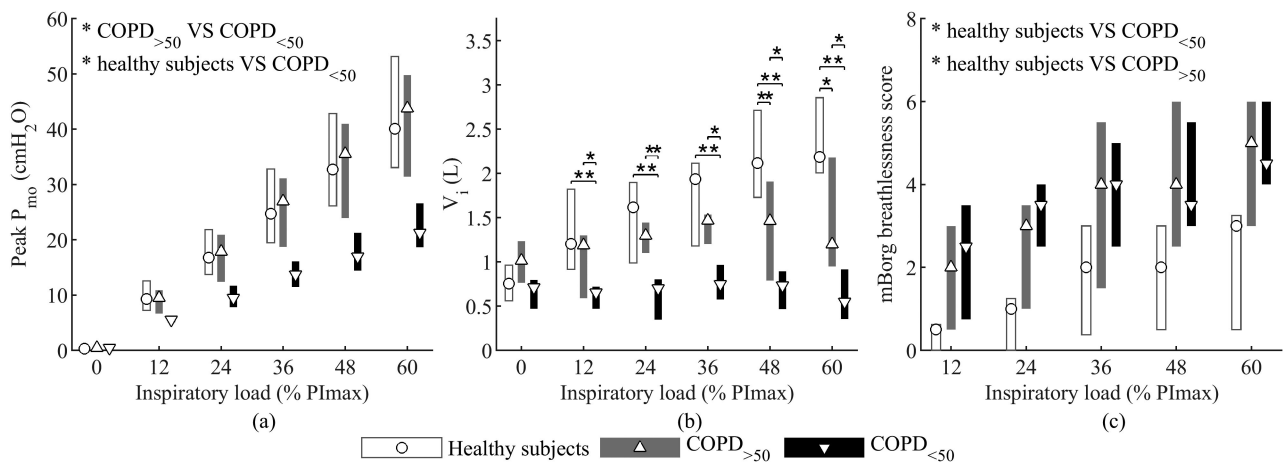


Fig. 1. Peak mouth pressure (P_{mo}) (a), inspiratory volume (V_i) (b), and modified Borg breathlessness score (mBorg) (c) during inspiratory threshold loading in healthy subjects and chronic obstructive pulmonary disease patients with a forced expiratory volume in 1 second value greater than or equal to 50 % predicted (COPD_{>50}) or lower than 50 % predicted (COPD_{<50}). Symbols represent data medians and bars represent data interquartile ranges. Asterisks indicate statistically significant differences (* for p-value < 0.05 and ** for p-value < 0.01).

0.002), resting fSEsMMG_{para%max} ($r = -0.48$, $p = 0.02$), and resting fSEsMMG_{lic%max} ($r = -0.46$, $p = 0.02$) (Fig. 3).

NMC and NVC ratios were also different between healthy subjects and COPD patients. NMC_{MMG-para} was significantly higher in healthy subjects (1.6 (1.2-2.2)) compared to both COPD_{<50} (0.8 (0.5-1.2), $p < 0.001$) and COPD_{>50} (1.0 (0.7-1.3), $p < 0.001$) patients during resting breathing. There were also significant differences ($p < 0.01$ in all cases) in NVC_{para} and NVC_{lic} between healthy subjects (0.08 (0.06-0.11) and 0.09 (0.07-0.11), respectively), COPD_{>50} patients (0.05 (0.04-0.06) and 0.04 (0.04-0.06), respectively), and COPD_{<50} patients (0.02 (0.02-0.02) and 0.02 (0.01-0.03), respectively).

Significant positive correlations were observed at rest (see Fig. 9 in the Appendix) between FEV₁% predicted and NMC_{MMG-para} ($r = 0.45$, $p = 0.02$), NMC_{MMG-lic} ($r = 0.42$, $p = 0.04$), NMC_{P-para} ($r = 0.44$, $p = 0.03$), MEff_{V-para} ($r = 0.53$, $p = 0.006$), MEff_{V-lic} ($r = 0.55$, $p = 0.004$), NVC_{para} ($r = 0.61$, $p = 0.001$), and NVC_{lic} ($r = 0.70$, $p < 0.001$).

2) *Inspiratory Muscle Activity During Inspiratory Threshold Loading:* fSEsMMG_{para%max}, fSEsMMG_{lic%max},

fSEsEMG_{para%max}, and fSEsEMG_{lic%max} values increased progressively at each successive stage of the inspiratory threshold loading protocol in healthy subjects and in COPD patients (Fig. 4a-4d). Strong to very strong positive correlations were obtained between fSEsEMG_{para%max} and fSEsMMG_{para%max} ($r = 0.8$, $p < 0.001$), and between fSEsEMG_{lic%max} and fSEsMMG_{lic%max} ($r = 0.78$, $p < 0.001$) (Fig. 4e and 4f respectively).

In healthy subjects, the transition from the baseline resting breathing to the first inspiratory load (12 % P_{max}) was associated with a proportionately greater increase in fSEsEMG_{para%max} compared to fSEsMMG_{para%max}. A corresponding significant decrease in NMC_{MMG-para} during the transition from rest to 12 % P_{max} (Fig. 4g) was seen. Subsequent, increases in fSEsMMG_{para%max} were in proportion to increases in fSEsEMG_{para%max} between successive inspiratory loads and only small, nonsignificant changes in NMC_{MMG-para} from 12 % to 60 % P_{max} were seen.

By contrast, in COPD_{<50} and COPD_{>50} patients, fSEsMMG_{para%max} increased in proportion to increases

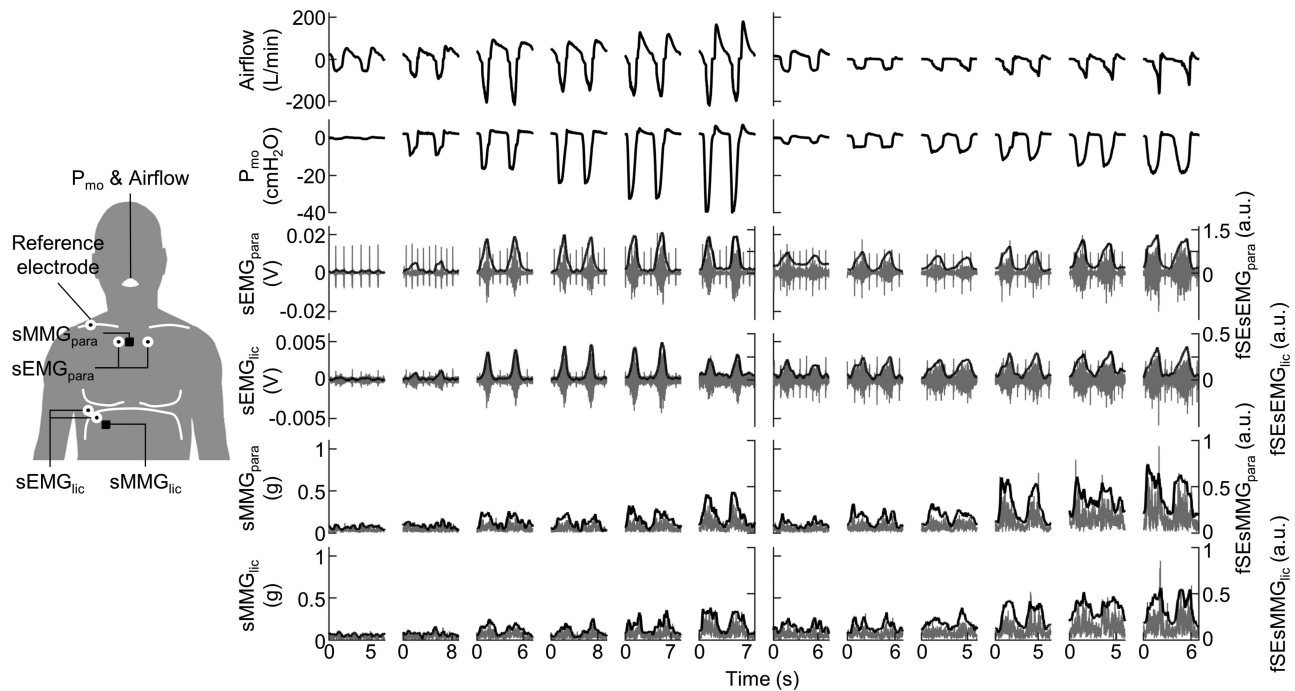


Fig. 2. Sensor positioning for data acquisition. Representative recordings in a healthy subject (left) and a chronic obstructive pulmonary disease patient (right) with a forced expiratory volume in 1 second value of less than 50 % predicted. Top to bottom: airflow, mouth pressure (P_{mo}), second intercostal space surface electromyography ($sEMG_{para}$), lower intercostal space surface electromyography ($sEMG_{lic}$), second intercostal space surface mechanomyography ($sMMG_{para}$), and lower intercostal space surface mechanomyography ($sMMG_{lic}$). Two respiratory cycles are shown for quiet resting breathing and inspiratory threshold loading at 12 %, 24 %, 36 %, 48 %, and 60 % P_{Imax} . Negative flow values correspond to inspiratory phases. Fixed sample entropy time-series are shown for the myographic signals ($fSEsEMG_{para}$, $fSEsEMG_{lic}$, $fSEsMMG_{para}$, and $fSEsMMG_{lic}$).

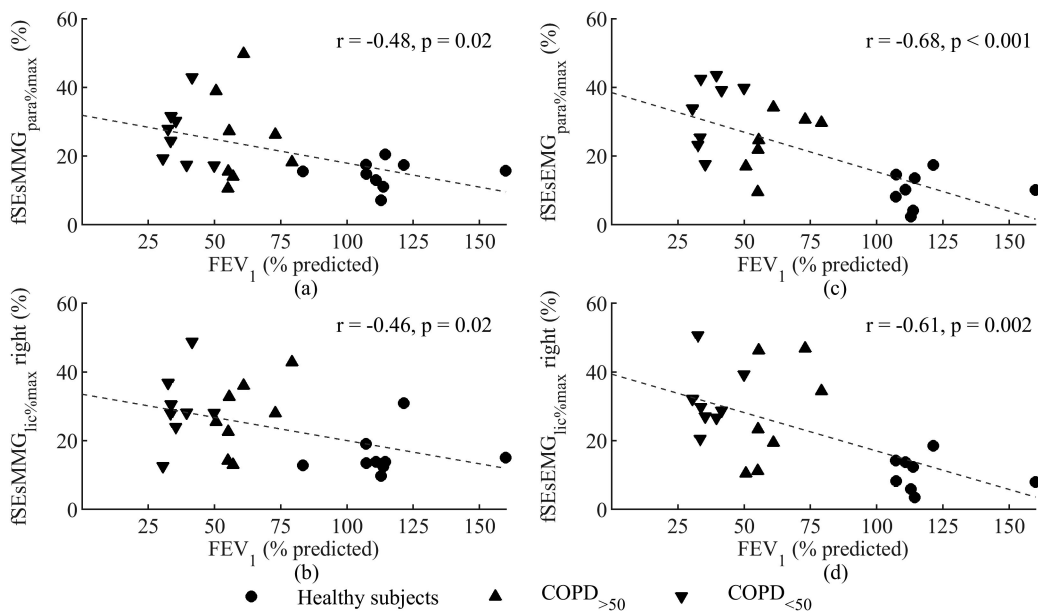


Fig. 3. Relationship between forced expiratory volume in 1 second (FEV_1) and normalized mean fixed sample entropy of surface mechanomyography and electromyography recorded over the second intercostal space ($fSEsMMG_{para\%max}$ and $fSEsEMG_{para\%max}$, respectively) (a and c) and over lower intercostal spaces ($fSEsMMG_{lic\%max}$ and $fSEsEMG_{lic\%max}$, respectively) (b and d) during resting breathing, in healthy subjects and chronic obstructive pulmonary disease patients with a FEV_1 value greater than or equal to 50 % predicted ($COPD_{>50}$) or lower than 50 % predicted ($COPD_{<50}$). Normalization was performed using the FEV_1 value obtained during either the inspiratory threshold loading protocol, the P_{Imax} maneuver, or the inspiratory lung capacity maneuver. Simple linear regression analysis was performed for each relationship.

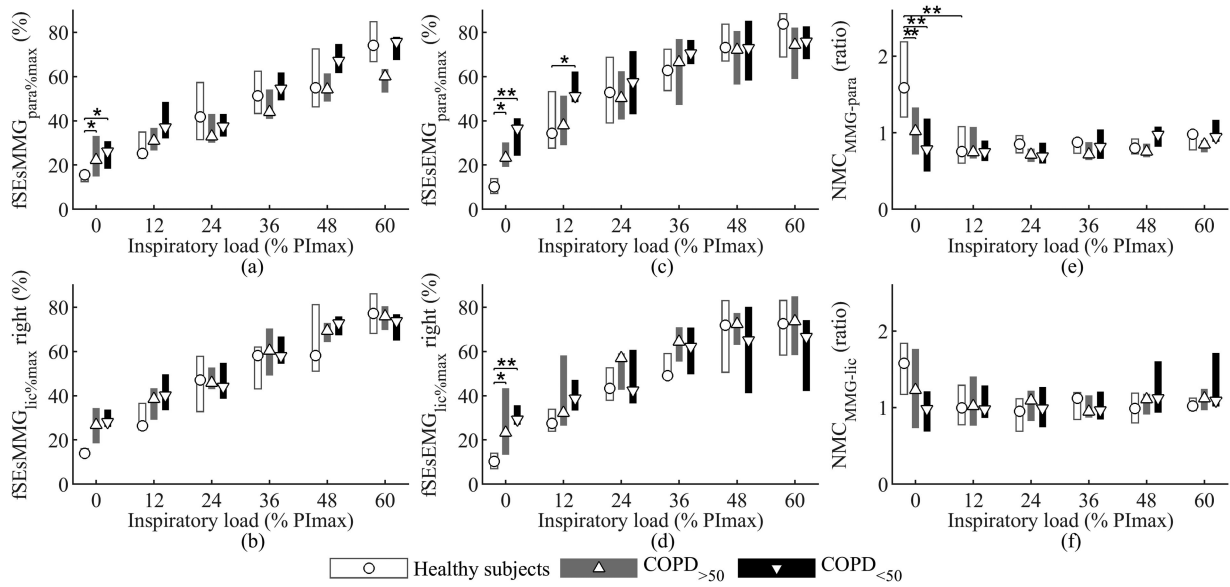


Fig. 4. Inspiratory muscle activity, measured as normalized mean fixed sample entropy of surface mechanomyography and electromyography recorded over the second intercostal space ($fSEsMMG_{para\%max}$ and $fSEsEMG_{para\%max}$, respectively) (a and c) and over lower intercostal spaces ($fSEsMMG_{lic\%max}$ and $fSEsEMG_{lic\%max}$, respectively) (b and d) during inspiratory threshold loading, in healthy subjects and chronic obstructive pulmonary disease patients with a forced expiratory volume in 1 second value greater than or equal to 50 % predicted ($COPD_{>50}$) or lower than 50 % predicted ($COPD_{<50}$). Normalization was performed using the largest values obtained during either the inspiratory threshold loading protocol, the P_{Imax} maneuver, or the inspiratory lung capacity maneuver. Relationship between sEMG- and sMMG-derived measures of inspiratory muscle activity (e and f). Inspiratory muscle neuromechanical coupling, measured as the ratios of $fSEsMMG_{para\%max}$ to $fSEsEMG_{para\%max}$ ($NMC_{MMG-para}$) (g) and $fSEsMMG_{lic\%max}$ to $fSEsEMG_{lic\%max}$ ($NMC_{MMG-lic}$) (h). Symbols represent data medians and bars represent data interquartile ranges. Asterisks indicate statistically significant differences (* for p-value < 0.05 and ** for p-value < 0.01).

in $fSEsEMG_{para\%max}$ both during the transition from rest to the first inspiratory load and during successive inspiratory loads up to 60 % P_{Imax} . Variations in $NMC_{MMG-para}$ across successive stages of the inspiratory threshold loading protocol were therefore small and nonsignificant (Fig. 4g).

There were no significant variations in $NMC_{MMG-lic}$ between different stages of the inspiratory threshold loading protocol in either healthy subjects or COPD patients (Fig. 4h). There were also no significant differences in $NMC_{MMG-para}$ or $NMC_{MMG-lic}$ between healthy controls and COPD patients during threshold loading.

The P_{mo} -derived ratios for myographic signals recorded over the second intercostal space, i.e., $MEff_{P-para}$ and NMC_{P-para} , were significantly lower in $COPD_{<50}$ patients than in $COPD_{>50}$ patients during threshold loading (Fig. 5a and 5c). $MEff_{P-para}$ was also significantly lower in $COPD_{<50}$ patients than in healthy subjects. Similar trends were observed for $MEff_{P-lic}$ and NMC_{P-lic} (Fig. 5b and 5d), but differences between $COPD_{<50}$ patients and either healthy subjects or $COPD_{>50}$ patients were less marked for signals recorded over lower intercostal spaces than for signals recorded over the second intercostal space. The lower P_{mo} -derived ratios observed in $COPD_{<50}$ patients compared to $COPD_{>50}$ patients and healthy subjects reflected the higher amount of NRD these patients needed to generate a given amount of inspiratory pressure (see Fig. 10 in the Appendix).

$COPD_{<50}$ patients also had significantly lower V_i -derived ratios for myographic signals recorded over the second intercostal space, i.e., $MEff_{V-para}$ and NVC_{para} , than $COPD_{>50}$ patients and healthy subjects during threshold loading (Fig. 6a

and 6c). For signals recorded over lower intercostal spaces, there were significant differences in $MEff_{V-lic}$ and NVC_{lic} between all groups (Fig. 6b and 6d).

Strong to very strong positive correlations were found between sEMG-derived indices of NMC and NVC (i.e., NMC_{P-para} , NMC_{P-lic} , NVC_{para} , and NVC_{lic}) and the corresponding sMMG-derived indices of MEff (i.e., $MEff_{P-para}$, $MEff_{P-lic}$, $MEff_{V-para}$, and $MEff_{V-lic}$) (Fig. 7).

IV. DISCUSSION

This is the first study to use a combination of surface electromyography and surface mechanomyography to compare neuromechanical coupling, neuroventilatory coupling, and mechanical efficiency of the chest wall respiratory muscles in COPD and in health in a wholly noninvasive manner. This is also the first study to describe the use of parasternal second intercostal space mechanomyography to quantify the load on the respiratory muscles in COPD. A glossary of abbreviations is included in Table I (Appendix).

$fSEsMMG_{para\%max}$, $fSEsEMG_{para\%max}$, and $fSEsEMG_{lic\%max}$ were significantly higher in COPD patients compared to values recorded in healthy subjects at rest, and there was a significant inverse correlation between $FEV_1\%$ predicted and $fSEsEMG_{para\%max}$, $fSEsEMG_{lic\%max}$, $fSEsMMG_{para\%max}$, and $fSEsMMG_{lic\%max}$. $NMC_{MMG-para}$, but not $NMC_{MMG-lic}$, was significantly higher in healthy subjects than in COPD patients at rest, and there were no significant differences between groups in $NMC_{MMG-para}$ or in $NMC_{MMG-lic}$ at inspiratory loads equivalent to between

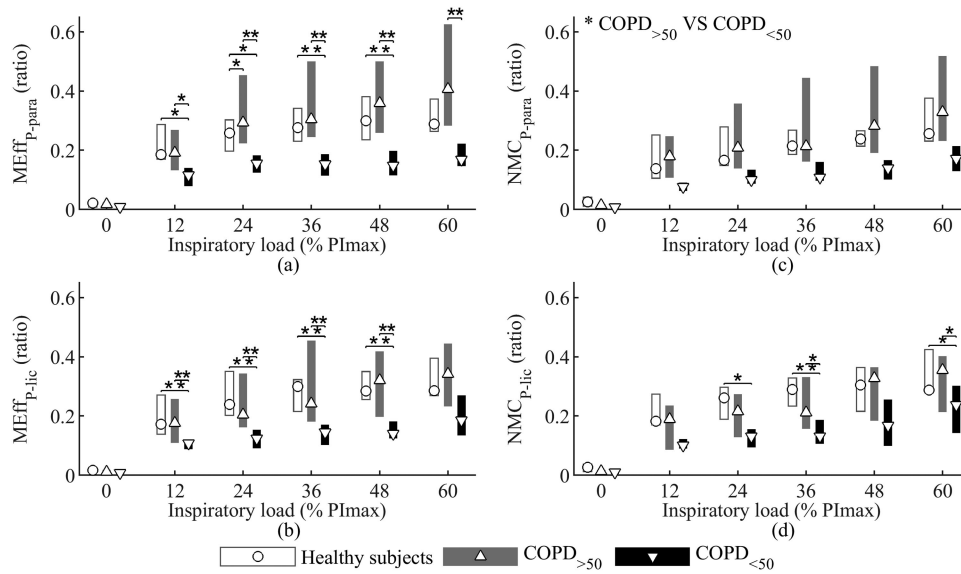


Fig. 5. Inspiratory muscle mechanical efficiency and neuromechanical coupling, measured as the ratios of mean mouth pressure to normalized mean fixed sample entropy of surface mechanomyography and electromyography, respectively (a and c) and over lower intercostal spaces (MEff_{P-lic} and NMC_{P-lic}, respectively) (b and d) during inspiratory threshold loading, in healthy subjects and chronic obstructive pulmonary disease patients with a forced expiratory volume in 1 second value greater than or equal to 50 % predicted (COPD_{>50}) or lower than 50 % predicted (COPD_{<50}). Symbols represent data medians and bars represent data interquartile ranges. Asterisks indicate statistically significant differences (* for p-value < 0.05 and ** for p-value < 0.01).

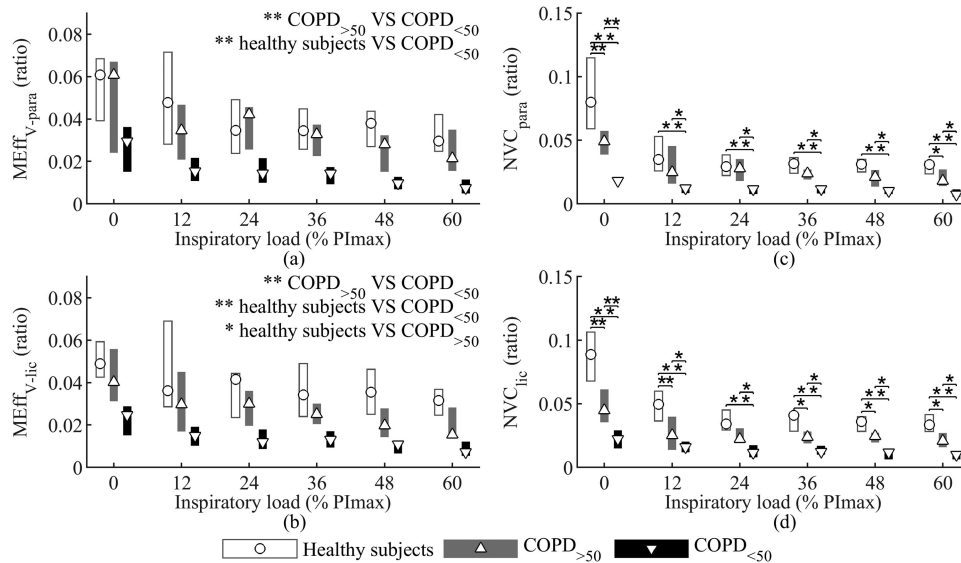


Fig. 6. Inspiratory muscle mechanical efficiency and neuroventilatory coupling, measured as the ratios of inspiratory volume to normalized mean fixed sample entropy of surface mechanomyography and electromyography, respectively, recorded over the second intercostal space (MEff_{V-para} and NVC_{para}, respectively) (a and c) and over lower intercostal spaces (MEff_{V-lic} and NVC_{lic}, respectively) (b and d) during inspiratory threshold loading, in healthy subjects and chronic obstructive pulmonary disease patients with a forced expiratory volume in 1 second value greater than or equal to 50 % predicted (COPD_{>50}) or lower than 50 % predicted (COPD_{<50}). Symbols represent data medians and bars represent data interquartile ranges. Asterisks indicate statistically significant differences (* for p-value < 0.05 and ** for p-value < 0.01).

12 % and 60 % PImax. During the inspiratory threshold loading protocol, P_{mo}-derived ratios of neuromechanical coupling and mechanical efficiency were lower in severe COPD patients (FEV₁ < 50 % predicted) than in moderate COPD patients (FEV₁ ≥ 50 % predicted) or healthy subjects, but differences were not consistently significant. V_i-derived

ratios of neuroventilatory coupling and mechanical efficiency, however, were consistently and significantly lower in severe COPD patients than in moderate COPD patients or healthy subjects during resting breathing and the inspiratory threshold loading protocol. Although the trends observed in these ratios were similar for recordings from the second intercostal space

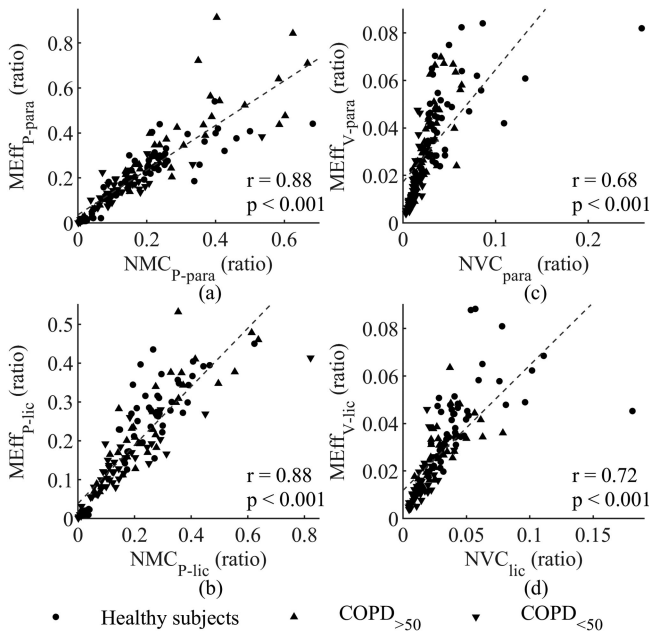


Fig. 7. Relationship between surface electromyography-derived ratios of neuromechanical (NMC_{P-para} and NMC_{P-lic}) or neuroventilatory (NVC_{para} and NVC_{lic}) coupling and surface mechanomyography-derived ratios of mechanical efficiency ($MEff_{P-para}$, $MEff_{P-lic}$, $MEff_{V-para}$, and $MEff_{V-lic}$) during inspiratory threshold loading, in healthy subjects and chronic obstructive pulmonary disease patients with a forced expiratory volume in 1 second value greater than or equal to 50 % predicted ($COPD_{>50}$) or lower than 50 % predicted ($COPD_{<50}$). Simple linear regression analysis was performed for each relationship.

and recordings from lower intercostal spaces, there were slight differences between the two locations. While between-group differences in P_{mo} -derived ratios were more consistently observed using recordings from the second intercostal space, i.e., $sEMG_{para}$ and $sMMG_{para}$, differences in V_i -derived ratios were more marked using recordings from the lower intercostal spaces, i.e., $sEMG_{lic}$ and $sMMG_{lic}$.

The use of respiratory muscle electromyography to derive quantitative indices of NRD is well-described in the literature. The observation that $fSEsEMG_{para\%max}$ and $fSEsEMG_{lic\%max}$ are higher in COPD than in healthy subjects is consistent with previous work using complementary methodology. Jolley *et al.* showed that crural diaphragm electromyographic activity measured using an esophageal multipair electrode catheter and analyzed using root mean square rather than $fSampEn$, was higher in COPD than in healthy individuals, with significant relationships between electromyographic measures, spirometric indices of airway obstruction, and lung hyperinflation [17]. Duiverman *et al.* measured overall inspiratory muscle activity in COPD and healthy individuals during an inspiratory loading protocol by adding the logarithm of the $sEMG$ activity ratio of the frontal diaphragm, the dorsal diaphragm, the intercostal muscles, and the left scalene muscle [20]. The $sEMG$ activity ratio of each specific muscle was calculated as the log ratio of the mean peak-to-peak inspiratory activity during threshold loading and the mean peak-to-peak value at baseline. Total

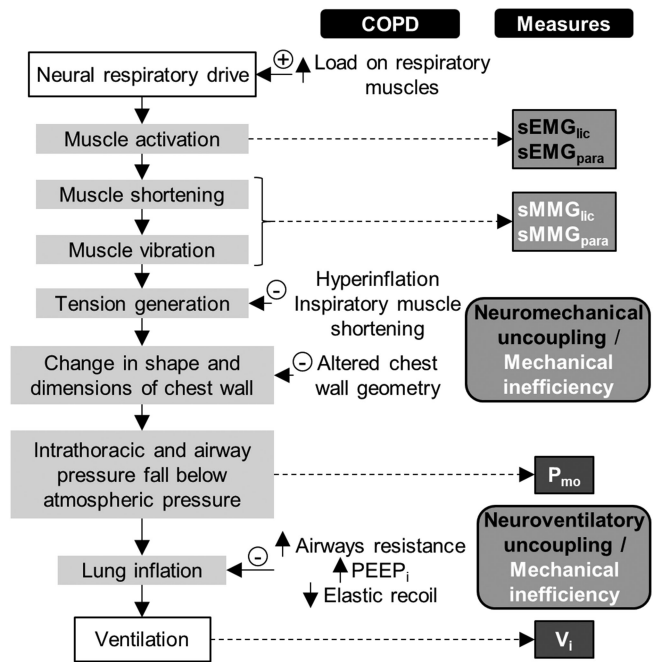


Fig. 8. Effect of chronic obstructive pulmonary disease (COPD) on the translation of neural respiratory drive to ventilation. Altered respiratory mechanics in COPD patients causes neuromechanical and neuroventilatory uncoupling and mechanical inefficiency, which can be quantified by measuring the electrical ($sEMG_{lic}$ and $sEMG_{para}$) and mechanical ($sMMG_{lic}$ and $sMMG_{para}$) activity of second intercostal and lower intercostal muscles, mouth pressure (P_{mo}), and inspiratory volume (V_i).

inspiratory muscle activity was found to be significantly higher in COPD than in healthy subjects at the lowest inspiratory threshold load (7 cmH₂O) only. Levels of $sEMG_{para}$ activity were also significantly higher in COPD patients compared with healthy subjects at the lowest load. Lin *et al.* reported that resting levels of NRD quantified from $sEMG_{para}$ and $sEMG_{lic}$ signals converted to root mean square were significantly higher in COPD patients than in healthy subjects [21]. Although not directly compared to values in healthy subjects, we have recently reported increasing values of mean $fSEsEMG_{lic}$ with increasing COPD severity during an inspiratory threshold loading protocol [22]. Moreover, $sEMG_{para}$ activity has been observed to track clinical progress during recovery from COPD exacerbations in hospitalized patients [3], [23]. These findings are consistent with the hypothesis that $sEMG_{para}$ and $sEMG_{lic}$ provide noninvasive indices of respiratory muscle load-capacity balance and NRD that are sensitive to impaired respiratory mechanics in COPD.

Although $sMMG$ is the mechanical counterpart of motor unit electrical activity as measured by $sEMG$ [24], it has been scarcely used to assess respiratory muscle function. In previous work, we have demonstrated strong correlations between P_{di} and mean $fSEsMMG_{lic}$ in healthy subjects during an incremental inspiratory muscle loading protocol, suggesting that $sMMG_{lic}$ could potentially provide a useful noninvasive alternative to P_{di} for the assessment of inspiratory muscle function [6]. The efficiency of mechanical activation of inspiratory muscles,

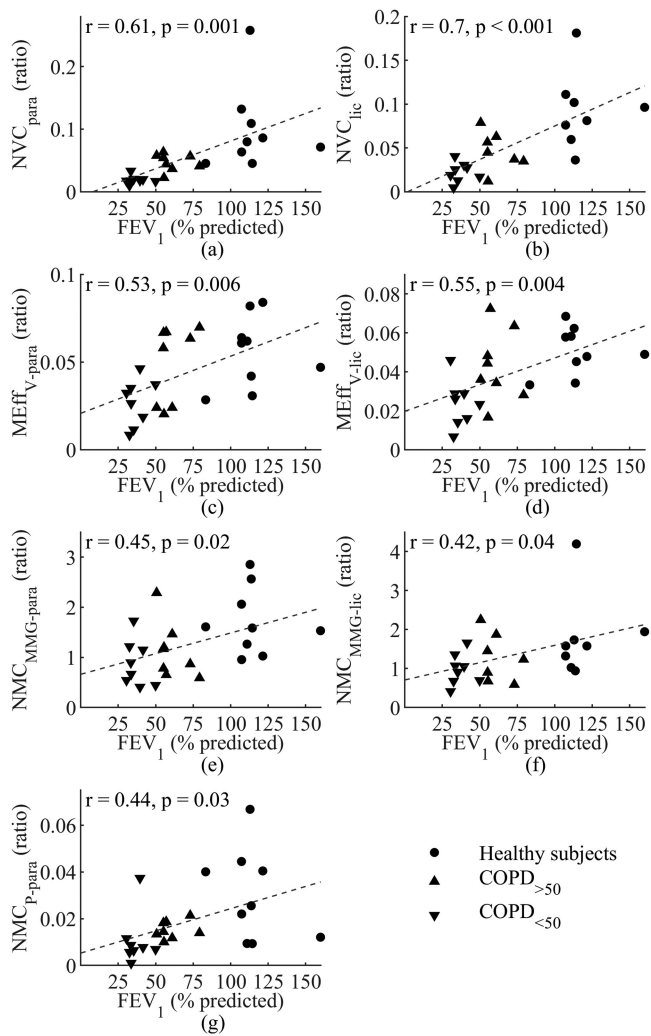


Fig. 9. Relationship between forced expiratory volume in 1 second (FEV₁) and indices of neuroventilatory coupling (NVC) (a and b), mechanical efficiency (MEff) (c and d), and neuromechanical coupling (NMC) (e, f, and g), in healthy subjects and chronic obstructive pulmonary disease patients with a FEV₁ value greater than or equal to 50 % predicted (COPD_{>50}) or lower than 50 % predicted (COPD_{<50}). Simple linear regression analysis was performed for each relationship.

measured as the ratio between peak inspiratory pressure and fSEsMMG_{lic}, has been shown to be lower in COPD patients than in healthy subjects, decreasing with increasing COPD severity [7], [8]. Recently, the ratio of bioimpedance amplitude to mean fSEsMMG_{lic}, proposed as an alternative measure of the contribution of mechanical activation of inspiratory muscles to ventilation, has been found to decrease with increasing COPD severity [22]. Together with our observations using sMMG_{lic} and, for the first time, sMMG_{para}, these findings suggest that noninvasive inspiratory muscle mechanomyography can provide useful indices of the efficiency of mechanical activation of the inspiratory muscles in COPD. Indeed, the strong to very strong correlations found between sEMG and sMMG measurements during inspiratory loading suggest that sMMG_{lic} and sMMG_{para} may provide useful alternatives to sEMG_{lic} and sEMG_{para} as

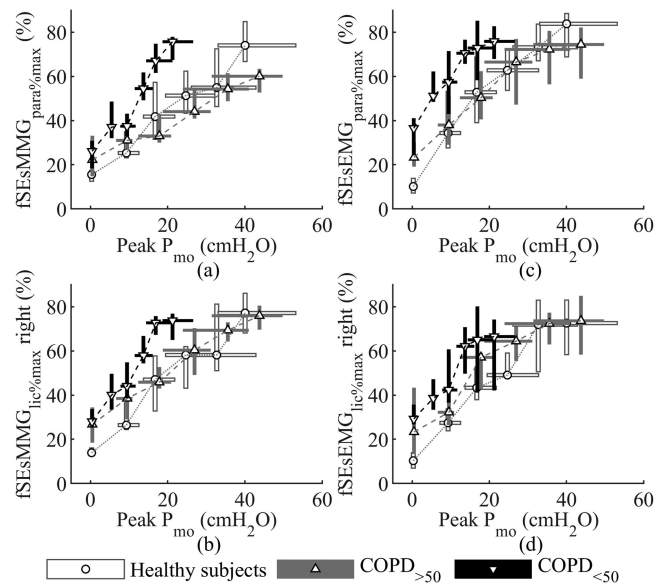


Fig. 10. Relationship between peak mouth pressure (P_{mo}) and inspiratory muscle activity, measured as normalized mean fixed sample entropy of surface mechanomyography and electromyography recorded over the second intercostal space (fSEsMMG_{para%}max and fSEsEMG_{para%}max, respectively) (a and c) and over lower intercostal spaces (fSEsMMG_{lic%}max and fSEsEMG_{lic%}max, respectively) (b and d) during inspiratory threshold loading, in healthy subjects and chronic obstructive pulmonary disease patients with a forced expiratory volume in 1 second value greater than or equal to 50 % predicted (COPD_{>50}) or lower than 50 % predicted (COPD_{<50}). Normalization was performed using the largest values obtained during either the inspiratory threshold loading protocol, the P_{lmax} maneuver, or the inspiratory lung capacity maneuver.

indices of NRD, as we have previously reported in healthy subjects [9], [10].

The relationship between sMMG and sEMG measurements represents the first step in the transformation of NRD into ventilation. Next steps, including the translation of respiratory muscle shortening and vibration into pressure, and the translation of pressure into ventilation, depend on several aspects, such as chest wall geometry, airways resistance, or lung compliance (Fig. 8). Our observations of similar NMC_{MMG-para} and NMC_{MMG-lic} ratios in healthy subjects and COPD patients, but impaired neuromechanical and neuroventilatory couplings (NMC_{P-para}, NMC_{P-lic}, NVC_{para}, and NVC_{lic}) and impaired mechanical efficiency (MEff_{P-para}, MEff_{P-lic}, MEff_{V-para}, and MEff_{V-lic}) in severe COPD patients suggest a disconnection between muscle activation/vibration (measured as sEMG and sMMG), muscle tension/pressure generation, and inspiratory airflow, caused by altered respiratory mechanics in COPD (Fig. 8). This suggests that sEMG and sMMG measures are not reliable indices of inspiratory muscle pressure generation in COPD. Since the two measures are muscle-specific (Fig. 8), sEMG and sMMG can be used to measure the uncoupling of inspiratory muscle activity from global mechanical output in COPD. Indeed, this has been demonstrated by the strong to very strong correlations found between sEMG- and sMMG-derived indices of NMC, NVC, and MEff. However, sMMG recordings have the advantage, over sEMG recordings, of not being

influenced by skin preparation, bioelectrical interference from other muscles, or by power line interference, which makes the evaluation of respiratory muscle function easier and faster to perform, and more acceptable in patients. Nevertheless, given the different nature of sEMG and sMMG signals, representing different stages of muscle activity, it is worthwhile to record both signals whenever possible, as their combination can provide relevant information about impaired inspiratory muscle function, such as the significant differences observed in this study in the resting $NMC_{MMG\text{-}para}$ between healthy subjects and COPD patients.

The use of fSampEn to analyze myographic signals is a relevant feature of this study. Since fSampEn values depend on signal complexity and signal amplitude, fSampEn can capture amplitude changes in sEMG and sMMG signals but is more robust against cardiac artefacts, since these are much less complex than sEMG and sMMG signals [5], [25]. Limitations of our study include the small sample size, but our findings form the basis for clinical validation studies in larger cohorts of COPD patients. Studies to define normative values of sMMG_{para} and sMMG_{lic} in healthy subjects are also required. The impact of dynamic operating lung volumes, which were not measured in this study, on the proposed noninvasive sEMG- and sMMG-derived indices should be also investigated in future studies, since it has been previously demonstrated that changes in operating lung volumes, especially end-inspiratory lung volume, affect inspiratory muscle activity and neuromechanical coupling [26]. Finally, sEMG_{lic} and sMMG_{lic} are not specific for the costal diaphragm and likely represent contribution of extradiaphragmatic chest wall and abdominal musculature, particularly during loaded breathing [6], [27]–[29]. sEMG_{para} and sMMG_{para} are similarly likely to represent contributions of upper chest wall and pectoral musculature, in addition to parasternal intercostal muscle myographic and mechanical activity, during loaded breathing [30], [31]. Identification of the costal diaphragm in the lower 7th/8th intercostal spaces is challenging and recording high quality sEMG_{lic} and sMMG_{lic} signals requires significant skill. However, the second intercostal space is more easily accessible, and sEMG_{para} and sMMG_{para} recordings, in comparison with sEMG_{lic} and sMMG_{lic}, are less influenced by chest wall thickness and subcutaneous fat [32], [33], and by crosstalk from postural chest wall and abdominal muscles [34], [35]. Therefore, it is relatively easier to acquire high quality sEMG and sMMG signals over the second intercostal space. The effect of BMI in sEMG and sMMG measures should however be a focus of future investigations.

The proposed noninvasive indices of NMC, NVC, and MEff have been tested at rest and during an inspiratory threshold loading protocol. These indices could be also of potential value to evaluate therapeutic interventions, such as inhaled bronchodilators, noninvasive ventilation, or inspiratory muscle training, aimed at reducing intrinsic respiratory mechanical loading in COPD patients [36]. Indeed, the efficiency of NRD, defined as the ratio of minute ventilation to the root mean square of invasive oesEMG_{di} measures, has been demonstrated to be a sensitive index to evaluate the response to inhaled bronchodilators in COPD, with significant improvements reported after bronchodilation

[37]. The application of the noninvasive indices proposed in this study in evaluating treatment benefits could therefore be a subject of future research.

V. CONCLUSION

The findings of this study suggest that sMMG_{lic} and, for the first time, sMMG_{para} are potential noninvasive alternatives to respiratory muscle electromyography for the assessment of NRD in COPD. The ratios of P_{mo} and V_i to sMMG and sEMG measurements provide indices of neuromechanical coupling, neuroventilatory coupling, and mechanical efficiency in COPD in a wholly noninvasive manner. These techniques are of potential value for the assessment of disease severity in clinical practice and provide useful and novel noninvasive research tools for the study of respiratory mechanics and respiratory muscle function in health and disease.

APPENDIX

TABLE II
GLOSSARY OF ABBREVIATIONS

Acronym	Definition
AIC	Akaike information criterion
COPD	Chronic obstructive pulmonary disease
COPD _{≥50}	COPD patients with FEV ₁ ≥ 50% predicted
COPD _{<50}	COPD patients with FEV ₁ < 50% predicted
FEV ₁	Forced expiratory volume in 1 second
fSampEn	Fixed sample entropy
fSEsEMG _{para}	fSampEn time-series of sEMG _{para} , sMMG _{para} , sEMG _{lic} , and sMMG _{lic} signals
fSEsMMG _{para}	
fSEsEMG _{lic}	
fSEsMMG _{lic}	
fSEsEMG _{para%max}	Normalized mean inspiratory fSampEn values of sEMG _{para} , sMMG _{para} , sEMG _{lic} , and sMMG _{lic} signals
fSEsMMG _{para%max}	
fSEsEMG _{lic%max}	
fSEsMMG _{lic%max}	
FVC	Forced vital capacity
mBorg	Modified Borg breathlessness score
MEff	Mechanical efficiency
MEff _{p-para}	mean P_{mo} / fSEsMMG _{para%max}
MEff _{p-lic}	mean P_{mo} / fSEsMMG _{lic%max}
MEff _{v-para}	V_i / fSEsMMG _{para%max}
MEff _{v-lic}	V_i / fSEsMMG _{lic%max}
mMRC	Modified British Medical Research Council
NMC	Neuromechanical coupling
NMC _{MMG-para}	fSEsMMG _{para%max} / fSEsEMG _{para%max}
NMC _{MMG-lic}	fSEsMMG _{lic%max} / fSEsEMG _{lic%max}
NMC _{p-para}	mean P_{mo} / fSEsEMG _{para%max}
NMC _{p-lic}	mean P_{mo} / fSEsEMG _{lic%max}
NRD	Neural respiratory drive
NVC	Neuroventilatory coupling
NVC _{para}	V_i / fSEsEMG _{para%max}
NVC _{lic}	V_i / fSEsEMG _{lic%max}
oesEMG _{di}	Esophageal crural diaphragm electromyography
P _{di}	Transdiaphragmatic pressure
PI _{max}	Maximal static inspiratory pressure
P _{mo}	Mouth pressure
sEMG	Surface electromyography
sMMG	Surface mechanomyography
sEMG _{para}	sEMG and sMMG recorded over parasternal second intercostal space
sMMG _{para}	
sEMG _{lic}	sEMG and sMMG recorded over lower intercostal spaces
sMMG _{lic}	
V _i	Inspiratory volume

ACKNOWLEDGMENT

The authors wish to thank the staff working in the Chest Unit at King's College Hospital and in the Chest Clinic at Guy's Hospital (London, U.K.) for making the lung function measurements and helping with patient recruitment.

Authors' Affiliations

Manuel Lozano-García is with the Universitat Politècnica de Catalunya (UPC)-Barcelona Tech, 08019 Barcelona, Spain, and also with the CIBER-BBN and Institute for Bioengineering of Catalonia (IBEC), The Barcelona Institute of Science and Technology (BIST), 08019 Barcelona, Spain (e-mail: mlozano@ibecbarcelona.eu).

Luis Estrada-Petrocelli is with the CIBER-BBN and Institute for Bioengineering of Catalonia (IBEC), The Barcelona Institute of Science and Technology (BIST), 08019 Barcelona, Spain, and also with Universidad Latina de Panamá, 0801 Panama City, Panama (e-mail: lestrada@ibecbarcelona.eu).

Dolores Blanco-Almazán is with the Universitat Politècnica de Catalunya (UPC)-Barcelona Tech, 08019 Barcelona, Spain, and also with the CIBER-BBN and Institute for Bioengineering of Catalonia (IBEC), The Barcelona Institute of Science and Technology (BIST), 08019 Barcelona, Spain (e-mail: dblanco@ibecbarcelona.eu).

Basak Tas is with the National Addiction Centre, Institute of Psychiatry, Psychology & Neuroscience (IoPPN), King's College London, WC2R 2LS London, U.K. (e-mail: basak.tas@kcl.ac.uk).

Peter S. P. Cho is with the Centre for Human & Applied Physiological Sciences, School of Basic & Medical Biosciences, Faculty of Life Sciences & Medicine, King's College London, King's Health Partners, WC2R 2LS London, U.K., and also with King's College Hospital NHS Foundation Trust, SE59RS, King's Health Partners, WC2R 2LS London, U.K. (e-mail: p.cho@nhs.net).

John Moxham is with the Centre for Human & Applied Physiological Sciences, School of Basic & Medical Biosciences, Faculty of Life Sciences & Medicine, King's College London, King's Health Partners, WC2R 2LS London, U.K. (e-mail: john.moxham@kcl.ac.uk).

Gerrard F. Rafferty is with the Centre for Human & Applied Physiological Sciences, School of Basic & Medical Biosciences, Faculty of Life Sciences & Medicine, King's College London, King's Health Partners, WC2R 2LS London, U.K. (e-mail: gerrard.rafferty@kcl.ac.uk).

Abel Torres and Raimon Jané are with the Universitat Politècnica de Catalunya (UPC)-Barcelona Tech, 08019 Barcelona, Spain, and also with the CIBER-BBN and Institute for Bioengineering of Catalonia (IBEC), The Barcelona Institute of Science and Technology (BIST), 08019 Barcelona, Spain (e-mail: abel.torres@upc.edu; rjane@ibecbarcelona.eu).

Caroline J. Jolley is with the Centre for Human & Applied Physiological Sciences, School of Basic & Medical Biosciences, Faculty of Life Sciences & Medicine, King's College London, King's Health Partners, WC2R 2LS London, U.K., and also with King's College Hospital NHS Foundation Trust, King's Health Partners, WC2R 2LS London, U.K. (e-mail: caroline.jolley@kcl.ac.uk).

REFERENCES

- [1] P. Laveneziana *et al.*, "ERS statement on respiratory muscle testing at rest and during exercise," *Eur. Respir. J.*, vol. 53, no. 6, Jun. 2019, Art. no. 1801214.
- [2] C. C. Reilly, C. J. Jolley, K. Ward, V. MacBean, J. Moxham, and G. F. Rafferty, "Neural respiratory drive measured during inspiratory threshold loading and acute hypercapnia in healthy individuals," *Exp. Physiol.*, vol. 98, no. 7, pp. 1190–1198, 2013.
- [3] E. S. Suh *et al.*, "Neural respiratory drive predicts clinical deterioration and safe discharge in exacerbations of COPD," *Thorax*, vol. 70, no. 12, pp. 1123–1130, Dec. 2015.
- [4] L. Smith *et al.*, "Physiological markers of exercise capacity and lung disease severity in cystic fibrosis," *Respirology*, vol. 22, no. 4, pp. 714–720, May 2017.
- [5] L. Estrada, A. Torres, L. Sarlabous, and R. Jané, "Improvement in neural respiratory drive estimation from diaphragm electromyographic signals using fixed sample entropy," *IEEE J. Biomed. Health Informat.*, vol. 20, no. 2, pp. 476–485, Mar. 2016.
- [6] M. Lozano-García *et al.*, "Surface mechanomyography and electromyography provide non-invasive indices of inspiratory muscle force and activation in healthy subjects," *Sci. Rep.*, vol. 8, no. 1, Dec. 2018, Art. no. 16921.
- [7] L. Sarlabous, A. Torres, J. A. Fiz, J. Gea, J. M. Martínez-Llorens, and R. Jané, "Efficiency of mechanical activation of inspiratory muscles in COPD using sample entropy," *Eur. Respir. J.*, vol. 46, no. 6, pp. 1808–1811, 2015.
- [8] L. Sarlabous, A. Torres, J. A. Fiz, J. M. Martínez-Llorens, J. Gea, and R. Jané, "Inspiratory muscle activation increases with COPD severity as confirmed by non-invasive mechanomyographic analysis," *PLoS One*, vol. 12, no. 5, May 2017, Art. no. e0177730.
- [9] M. Lozano-García *et al.*, "Noninvasive assessment of neuromechanical coupling and mechanical efficiency of parasternal intercostal muscle during inspiratory threshold loading," *Sensors*, vol. 21, no. 5, pp. 1–15, Mar. 2021.
- [10] M. Lozano-García *et al.*, "Noninvasive assessment of inspiratory muscle neuromechanical coupling during inspiratory threshold loading," *IEEE Access*, vol. 7, pp. 183634–183646, 2019.
- [11] "Global initiative for chronic obstructive lung disease (GOLD). Global strategy for the diagnosis, management, and prevention of chronic obstructive pulmonary disease." 2021. [Online] Available: https://goldcopd.org/wp-content/uploads/2020/11/GOLD-REPORT-2021-v1.1-25Nov20_WMV.pdf
- [12] B. L. Graham *et al.*, "Standardization of spirometry 2019 update. An official American Thoracic Society and European Respiratory Society technical statement," *Amer. J. Respir. Crit. Care Med.*, vol. 200, no. 8, pp. e70–e88, Oct. 2019.
- [13] P. H. Quanjer *et al.*, "Multi-ethnic reference values for spirometry for the 3–95-yr age range: The global lung function 2012 equations," *Eur. Respir. J.*, vol. 40, no. 6, pp. 1324–1343, Dec. 2012.
- [14] D. A. Mahler and C. K. Wells, "Evaluation of clinical methods for rating dyspnea," *Chest*, vol. 93, no. 3, pp. 580–586, 1988.
- [15] V. MacBean, C. Hughes, G. Nicol, C. C. Reilly, and G. F. Rafferty, "Measurement of neural respiratory drive via parasternal intercostal electromyography in healthy adult subjects," *Physiol. Meas.*, vol. 37, no. 11, pp. 2050–2063, Nov. 2016.
- [16] M. Petitjean and F. Bellemare, "Phonomyogram of the diaphragm during unilateral and bilateral phrenic nerve stimulation and changes with fatigue," *Muscle Nerve*, vol. 17, no. 10, pp. 1201–1209, Oct. 1994.
- [17] C. J. Jolley *et al.*, "Neural respiratory drive in healthy subjects and in COPD," *Eur. Respir. J.*, vol. 33, no. 2, pp. 289–297, 2009.
- [18] G. A. Borg, "Psychophysical bases of perceived exertion," *Med. Sci. Sports Exercise*, vol. 14, no. 5, pp. 377–381, 1982.
- [19] M. Lozano-García, L. Estrada, and R. Jané, "Performance evaluation of fixed sample entropy in myographic signals for inspiratory muscle activity estimation," *Entropy*, vol. 21, no. 2, Feb. 2019, Art. no. 183.
- [20] M. L. Duiverman, L. A. van Eykern, P. W. Vennik, G. H. Koter, E. J. W. Maarsingh, and P. J. Wijkstra, "Reproducibility and responsiveness of a noninvasive EMG technique of the respiratory muscles in COPD patients and in healthy subjects," *J. Appl. Physiol.*, vol. 96, no. 5, pp. 1723–1729, 2004.
- [21] L. Lin, L. Guan, W. Wu, and R. Chen, "Correlation of surface respiratory electromyography with esophageal diaphragm electromyography," *Respir. Physiol. Neurobiol.*, vol. 259, pp. 45–52, Jan. 2019.
- [22] D. Blanco-Almazán *et al.*, "Combining bioimpedance and myographic signals for the assessment of COPD during loaded breathing," *IEEE Trans. Biomed. Eng.*, vol. 68, no. 1, pp. 298–307, Jan. 2021.
- [23] P. B. Murphy *et al.*, "Neural respiratory drive as a physiological biomarker to monitor change during acute exacerbations of COPD," *Thorax*, vol. 66, no. 7, pp. 602–608, Jul. 2011.
- [24] T. W. Beck *et al.*, "Mechanomyographic amplitude and mean power frequency versus torque relationships during isokinetic and isometric muscle actions of the biceps brachii," *J. Electromyography Kinesiol.*, vol. 14, no. 5, pp. 555–564, 2004.
- [25] L. Sarlabous, A. Torres, J. A. Fiz, and R. Jané, "Evidence towards improved estimation of respiratory muscle effort from diaphragm mechanomyographic signals with cardiac vibration interference using sample entropy with fixed tolerance values," *PLoS One*, vol. 9, no. 2, 2014, Art. no. e88902.
- [26] F. Niro, B. Dubuc, K. G. Sodeifi, and D. Jensen, "Effect of end-inspiratory lung volume and breathing pattern on neural activation of the diaphragm and extra-diaphragmatic inspiratory muscles in healthy adults," *J. Appl. Physiol.*, vol. 131, no. 6, pp. 1679–1690, Dec. 2021.
- [27] A. Demoule, E. Verin, C. Locher, J. P. Derenne, and T. Similowski, "Validation of surface recordings of the diaphragm response to transcranial magnetic stimulation in humans," *J. Appl. Physiol.*, vol. 94, no. 2, pp. 453–461, 2003.

- [28] M. Yokoba, T. Abe, M. Katagiri, T. Tomita, and P. A. Easton, "Respiratory muscle electromyogram and mouth pressure during isometric contraction," *Respir. Physiol. Neurobiol.*, vol. 137, no. 1, pp. 51–60, Aug. 2003.
- [29] A. H. Ramsook *et al.*, "Diaphragm recruitment increases during a bout of targeted inspiratory muscle training," *Med. Sci. Sports Exercise*, vol. 48, no. 6, pp. 1179–1186, 2016.
- [30] V. R. Nepomuceno, E. M. Nepomuceno, S. C. H. Regalo, E. P. Cerqueira, and R. R. Souza, "Electromyographic study on the sternocleidomastoid and pectoralis major muscles during respiratory activity in humans," *J. Morphological Sci.*, vol. 31, no. 2, pp. 98–102, 2014.
- [31] A. H. Ramsook *et al.*, "Is parasternal intercostal EMG an accurate surrogate of respiratory neural drive and biomarker of dyspnea during cycle exercise testing?," *Respir. Physiol. Neurobiol.*, vol. 242, pp. 40–44, Aug. 2017.
- [32] J. C. Glerant *et al.*, "Diaphragm electromyograms recorded from multiple surface electrodes following magnetic stimulation," *Eur. Respir. J.*, vol. 27, no. 2, pp. 334–342, Feb. 2006.
- [33] I. M. M. Dos Reis, D. G. Ohara, L. B. Januário, R. P. Basso-Vanelli, A. B. Oliveira, and M. Jamami, "Surface electromyography in inspiratory muscles in adults and elderly individuals: A systematic review," *J. Electromyography Kinesiol.*, vol. 44, pp. 139–155, Jan. 2019.
- [34] C. Sinderby, S. Friberg, N. Comtois, and A. Grassino, "Chest wall muscle cross talk in canine costal diaphragm electromyogram," *J. Appl. Physiol.*, vol. 81, no. 5, pp. 2312–2327, 1996.
- [35] A. De Troyer, M. Estenne, V. Ninane, D. Van Gansbeke, and M. Gorini, "Transversus abdominis muscle function in humans," *J. Appl. Physiol.*, vol. 68, no. 3, pp. 1010–1016, 1990.
- [36] D. Jensen, M. R. Schaeffer, and J. A. Guenette, "Pathophysiological mechanisms of exertional breathlessness in chronic obstructive pulmonary disease and interstitial lung disease," *Curr. Opin. Supportive Palliat. Care*, vol. 12, no. 3, pp. 237–245, Sep. 2018.
- [37] Y. Li *et al.*, "Efficiency of neural respiratory drive for the assessment of bronchodilator responsiveness in patients with chronic obstructive pulmonary disease: An exploratory study," *J. Thoracic Dis.*, vol. 8, no. 5, pp. 958–965, May 2016.